1P5-2

Proceedings of Symposium on Ultrasonic Electronics, Vol. 35 (2014) pp. 127-128
3-5 December, 2014

Numerical Simulations of Piezoelectric Effect under Ultrasound Irradiation: For Analysis of Piezoelectric Effect of Bone

超音波照射下での圧電効果の数値シミュレーション:骨の圧電効果の解析に向けて

Atsushi Hosokawa† (Dept. Electr. & Comp. Eng., Nat. Inst. Tech., Akashi Coll.)
細川篤† (明石高専 電気情報)

1. Introduction

Bone remodeling, which comprises a coupling of bone formation and resorption due to osteoblastic and osteoclastic activities, can be driven by the mechanical load applied to the bone.[1] By applying this mechanism, the accelerated healing of bone fracture using low-intensity ultrasound has been practically used.[2] As the bone formation can accompany the piezoelectric effect of bone,[3] the piezoelectric effect under ultrasound irradiation should be sufficiently clarified in order to realize more effective healing.

Numerical simulations using an elastic finite-difference time-domain (FDTD) method can be a surrogate for experiments of ultrasound propagation in bone. For analyzing the pizoelectric effect of bone, the use of the elastic FDTD method with piezoelectric constitutive equations (refered to as piezoelectric FDTD method) was considered. In this study, the ultrasound propagations in the virtual bones with pseudovalues of the piezoelectric parameters were simulated using the piezoelectric FDTD method.

2. Elastic and Piezoelectric FDTD Methods

The ultrasound propagation in an isotropic elastic material is governed by the following partial differential equations:

$$\rho \frac{\partial \dot{u}_i}{\partial t} = \frac{\partial \tau_{ii}}{\partial x_i} + \frac{\partial \tau_{ij}}{\partial x_j} + \frac{\partial \tau_{ik}}{\partial x_k}, \quad (1)$$

$$\frac{\partial \tau_{ii}}{\partial t} = (\lambda + 2\mu)\frac{\partial \dot{u}_i}{\partial x_i} + \lambda \frac{\partial \dot{u}_j}{\partial x_j} + \lambda \frac{\partial \dot{u}_k}{\partial x_k}, \quad (2)$$

$$\frac{\partial \tau_{jk}}{\partial t} = \mu\left(\frac{\partial \dot{u}_j}{\partial x_k} + \frac{\partial \dot{u}_k}{\partial x_j}\right), \quad (3)$$

where $i, j, k = 1, 2, 3$. In these equations, $\dot{u}_i$ (dot denotes the time differentiation) is the particle velocity in the i–direction, τ_{ii} is the normal stress in the i–direction, τ_{jk} ($j \neq k$) is the shear stress on the j–k plane, ρ is the medium density, and λ and μ are the first and second Lamé coefficients, respectively. In the elastic FDTD method, the partial differentiations in Eqs. (1)–(3) are discretized using a central differencing scheme with staggered arrangements of $\dot{u}$ and τ in both spatial and temporal regions. The discrete values of $\dot{u}$ and τ in all spatial points, which are calculated using Eq. (1) and Eqs. (2) and (3), respectively, are alternatively updated every half time step.

The piezoelectric constitutive equations in stress-charge form are:

$$\tau_{ii} = (\lambda + 2\mu)\frac{\partial u_i}{\partial x_i} + \lambda \frac{\partial u_j}{\partial x_j} + \lambda \frac{\partial u_k}{\partial x_k} - e_{ii} E_i, \quad (4)$$

$$D_i = e_{ii} \frac{\partial u_i}{\partial x_i} + \varepsilon_{ii} E_i, \quad (5)$$

provided that e_{jk} and ε_{jk} ($j \neq k$) are assumed to be zero. E_i is the electric field, D_i is the electric displacement, e_{ii} is the piezoelectric constant, and ε_{ii} is the dielectric constant. The time derivatives of Eqs. (4) and (5) yield:

$$\frac{\partial \tau_{ii}}{\partial t} = (\lambda + 2\mu)\frac{\partial \dot{u}_i}{\partial x_i} + \lambda \frac{\partial \dot{u}_j}{\partial x_j} + \lambda \frac{\partial \dot{u}_k}{\partial x_k} - e_{ii} \frac{\partial E_i}{\partial t}, \quad (6)$$

$$\frac{\partial D_i}{\partial t} = e_{ii} \frac{\partial \dot{u}_i}{\partial x_i} + \varepsilon_{ii} \frac{\partial E_i}{\partial t}. \quad (7)$$

In the piezoelectric FDTD method, Eq. (6) is used instead of Eq. (2), and the discrete values of E are calculated using Eq. (7), together with the calculations of τ.

3. Simulated Results and Discussion

In this study, for two virtual bones with piezoelectric parameter values of lead titanate zirconate (PZT) and poly(vinylidene fluoride) (PVDF) in water, the FDTD simulations of the ultrasound propagations were performed. The whole region of the simulation model, that is the water region, was 38.5 × 24.5 × 24.5 mm, and a long bone was allocated in the middle of this region. The long bone was simplified as a tubular cylinder composing of human cortical bone, and its hollow was filled with water. The outer and inner diameters of the tube were 24 and 16 mm, respectively. The

hosokawa@akashi.ac.jp

Table I Elastic parameter values of cortical bone and water used in FDTD simulations.

	Cortical bone	Water
First Lamé coefficient λ (GPa)	17.6	2.2
Second Lamé coefficient μ (GPa)	6.0	0
Density ρ (kg/m^3)	1850	1000

Table II Piezoelectric parameter values of PZT and PVDF used in FDTD simulations.

	PZT	PVDF
Piezoelectric constant e (C/m^2)	15.1	-0.14
Dielectric constant ε ($\times 10^{-12}$ F/m)	5620	55

elastic properties of the long bone were homogeneous and isotropic, and the piezoelectric properties were given in the axial and radial directions. **Table I** lists the elastic parameter values of cortical bone and water used in the FDTD simulations, and **Table II** lists the piezoelectric parameter values of PZT and PVDF. The transmitting and receiving surfaces, whose diameters were 10 mm, were coaxially allocated at a distance of 38.5 mm across the long bone. A pulsed ultrasound wave with a center frequency of 1 MHz was transmitted in the radial direction of the bone. At all boundaries surrounding the simulation region, 20 perfectly matched absorbing layers (PMLs)[4] were set to prevent artificial reflections.

Figure 1 shows the simulated waveforms obtained using the piezoelectric FDTD method, in which the black and gray lines illustrate the waveforms propagating in the virtual bones with and without the piezoelectric properties, respectively. Noted that the gray waveforms corresponded to the waveforms obtained using the elastic FDTD method. Figures 1(a) and 1(b) show the waveforms for the bones with the piezoelectric properties of PZT and PVDF, respectively. Comparing between the black and gray waveforms in Fig. 1(a), the amplitude of the former waveform was smaller and the propagation time was shorter. In addition, their shapes greatly differed. These were considered to be because the elastic properties were equivalently changed by the piezoelectric properties. Thus, the piezoelectric effect of PZT on the ultrasound propagation could be observed.

In Fig. 1(b), the simulated waveforms for the bones with and without the PVDF properties were almost the same, and the piezoelectric effect could be hardly observed. Okino, *et al.*[5] reported that the voltage sensitivities of self-made transducers composing of bovine cortical bone were around 1/1000 of a PVDF transducer in MHz range. It was therefore considered that the piezoelectric effect in the actual bone could be little.

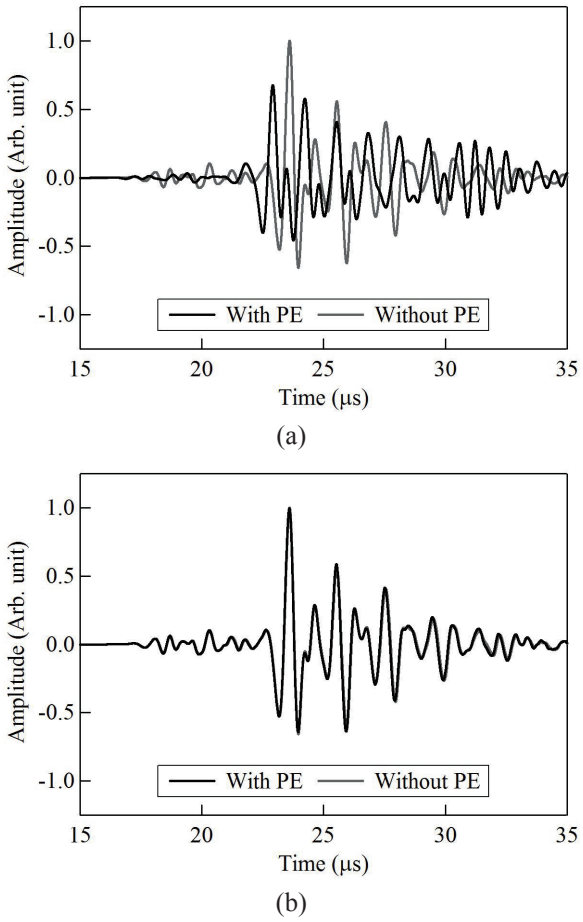

Fig. 1 Simulated waveforms propagating in virtual bones with and without piezoelectric (PE) properties of (a) PZT and (b) PVDF.

4. Conclusions

In this study, the piezoelectric effects on the ultrasound propagations in the virtual bones were simulated using the piezoelectric FDTD method. It was considered that the piezoelectric effect in the actual bone could be little.

Acknowledgment

Part of this study was supported by JSPS through a Grant-in-Aid for Scientific Research (B) (No. 24360161).

References

1. A. M. Parfitt: J. Cell. Biochem. **55** (1994) 273.
2. S. Mitragotri: Nat. Rev. Drug. Discovery **4** (2005) 255.
3. E. Fukuda and I. Yasuda: J. Phys. Soc. Jpn. **12** (1957) 1158.
4. W. C. Chew and Q. H. Liu: J. Comput. Acoust. **4** (1996) 341.
5. M. Okino, *et al.*: J. Appl. Phys. Lett. **103** (2013) 103701.